Int. Conference on Boundary and Interior Layers
BAIL 2006
G. Lube, G. Rapin (Eds)

Derivation of an adjoint consistent discontinuous Galerkin discretization of the compressible Euler equations

Ralf Hartmann

Institute of Aerodynamics and Flow Technology, German Aerospace Center (DLR),
Lilienthalplatz 7, 38108 Braunschweig, Germany, Ralf.Hartmann@dlr.de,
and Institute of Scientific Computing, TU Braunschweig

1. Introduction

Adjoint consistency - in addition to consistency - is the key requirement for discontinuous Galerkin (DG) discretizations to be of optimal order in L^2 as well as measured in terms of target functionals. Furthermore, adjoint consistency is closely related to the smoothness of discrete adjoint solutions. Whereas adjoint solutions based on the (non-adjoint-consistent) NIPG method are discontinuous between element interfaces, where the jumps in the adjoint solutions even persist as the mesh is refined, [4], the adjoint solutions based on the (adjoint-consistent) SIPG method are essentially continuous, see also [3] for an appropriate modification of a specific target functional for the Laplace equation. Furthermore, we also refer to the topic of asymptotic adjoint consistency of stabilized finite element methods, [8]. Recently, [9] proposed a specific discretization of the boundary fluxes and the target functional to recover an adjoint consistent DG discretization of the compressible Euler equations.

In this paper, we provide a general framework for analyzing adjoint consistency of DG discretizations and introduce so-called consistent modifications of target functionals in Section 2. Whereas the standard DG discretization of compressible Euler equations, e.g. [2, 6], is not adjoint consistent, we use the outlined framework to derive the adjoint consistent discretization of the compressible Euler equations proposed in [9]. Numerical experiments demonstrate the effect of adjoint consistency on the smoothness of discrete adjoint solutions and on the *a posteriori* error estimation on adaptively refined meshes. The developed framework is particularly useful for deriving adjoint consistent discretizations of more complex nonlinear problems, see [5].

2. Consistency and adjoint consistency

On an bounded open domain $\Omega \subset \mathbb{R}^d$ with boundary Γ we consider following nonlinear problem

$$N\mathbf{u} = 0 \quad \text{in } \Omega, \qquad\qquad B\mathbf{u} = \mathbf{g} \quad \text{on } \Gamma, \tag{1}$$

where N is a nonlinear differential (and Fréchet-differentiable) operator and B is a (possibly nonlinear) boundary operator. Let $J(\cdot)$ be a (nonlinear) target functional

$$J(\mathbf{u}) = \int_\Omega j_\Omega(\mathbf{u})\,\mathrm{d}\mathbf{x} + \int_\Gamma j_\Gamma(\mathbf{u})\,\mathrm{d}s, \tag{2}$$

with Fréchet derivative

$$J'[\mathbf{u}](\mathbf{w}) = \int_\Omega j'_\Omega[\mathbf{u}]\,\mathbf{w}\,\mathrm{d}\mathbf{x} + \int_\Gamma j'_\Gamma[\mathbf{u}]\,\mathbf{w}\,\mathrm{d}s,$$

where $j_\Omega(\cdot)$ and $j_\Gamma(\cdot)$ may be nonlinear with derivatives j'_Ω and j'_Γ. Here, $'$ denotes the Fréchet derivative and the square bracket $[\cdot]$ denotes the state about which linearization is performed. Then, the adjoint problem to (1) is given by

$$(N'[\mathbf{u}])^*\mathbf{z} = j'_\Omega[\mathbf{u}] \quad \text{in } \Omega, \qquad\qquad (B'[\mathbf{u}])^*\mathbf{z} = j'_\Gamma[\mathbf{u}] \quad \text{on } \Gamma, \tag{3}$$

where $(N'[\mathbf{u}])^*$ and $(B'[\mathbf{u}])^*$ denote the adjoint operators to $N'[\mathbf{u}]$ and $B'[\mathbf{u}]$, respectively. Let Ω be subdivided into shape-regular meshes $\mathcal{T}_h = \{\kappa\}$ consisting of elements κ and let $\mathbf{V}_h$ be a discrete function space on $\mathcal{T}_h$. Finally, let problem (1) be discretized as follows: Find $\mathbf{u}_h \in \mathbf{V}_h$ such that

$$\mathcal{N}(\mathbf{u}_h, \mathbf{v}) = 0 \quad \forall \mathbf{v} \in \mathbf{V}_h, \tag{4}$$

where $\mathcal{N}$ is a semi-linear form. Then, the discretization (4) is said to be *consistent* if the solution $\mathbf{u}$ to the primal problem (1) satisfies following equation:

$$\mathcal{N}(\mathbf{u}, \mathbf{v}) = 0 \quad \forall \mathbf{v} \in \mathbf{V}. \tag{5}$$

where $\mathbf{V}$ is an appropriately chosen function space. The discretization (4) is said to be *adjoint consistent* if the exact solution $\mathbf{z}$ to the adjoint problem (3) satisfies following equation:

$$\mathcal{N}'[\mathbf{u}](\mathbf{w}, \mathbf{z}) = J'[\mathbf{u}](\mathbf{w}) \quad \forall \mathbf{w} \in \mathbf{V}, \tag{6}$$

where $\mathcal{N}'[\mathbf{u}]$ denotes the Fréchet derivative of $\mathcal{N}$. In other words, a discretization is adjoint consistent if the associated discrete adjoint problem is a consistent discretization of the continuous adjoint problem. Finally, we note, that the definition in (6) of adjoint consistency for nonlinear problems, see also [9], generalizes the definition of (linear) adjoint consistency in that for linear problems and target functionals it reduces to the definition of (linear) adjoint consistency as given in e.g. [1].

For analyzing consistency of a discontinuous Galerkin discretization, we rewrite (4) in following primal residual form: Find $\mathbf{u}_h \in \mathbf{V}_h$ such that

$$\sum_{\kappa \in \mathcal{T}_h} \int_\kappa \mathbf{R}(\mathbf{u}_h) \cdot \mathbf{v} \, \mathrm{d}\mathbf{x} + \sum_{\kappa \in \mathcal{T}_h} \int_{\partial\kappa \setminus \Gamma} \mathbf{r}(\mathbf{u}_h) \cdot \mathbf{v} \, \mathrm{d}s + \int_\Gamma \mathbf{r}_\Gamma(\mathbf{u}_h) \cdot \mathbf{v} \, \mathrm{d}s = 0 \quad \forall \mathbf{v} \in \mathbf{V}_h, \tag{7}$$

where $\mathbf{R}(\mathbf{u}_h)$, $\mathbf{r}(\mathbf{u}_h)$ and $\mathbf{r}_\Gamma(\mathbf{u}_h)$ denote the element, interior face and boundary residuals, respectively. According to (5), the discretization is *consistent* if the exact solution $\mathbf{u}$ to (1) satisfies

$$\sum_{\kappa \in \mathcal{T}_h} \int_\kappa \mathbf{R}(\mathbf{u}) \cdot \mathbf{v} \, \mathrm{d}\mathbf{x} + \sum_{\kappa \in \mathcal{T}_h} \int_{\partial\kappa \setminus \Gamma} \mathbf{r}(\mathbf{u}) \cdot \mathbf{v} \, \mathrm{d}s + \int_\Gamma \mathbf{r}_\Gamma(\mathbf{u}) \cdot \mathbf{v} \, \mathrm{d}s = 0 \quad \forall \mathbf{v} \in \mathbf{V}, \tag{8}$$

which holds if $\mathbf{u}$ satisfies

$$\mathbf{R}(\mathbf{u}) = 0 \ \text{ in } \kappa, \kappa \in \mathcal{T}_h, \qquad \mathbf{r}(\mathbf{u}) = 0 \ \text{ on } \partial\kappa \setminus \Gamma, \kappa \in \mathcal{T}_h, \qquad \mathbf{r}_\Gamma(\mathbf{u}) = 0 \ \text{ on } \Gamma. \tag{9}$$

To analyze adjoint consistency, we rewrite the discrete adjoint problem: Find $\mathbf{z}_h \in \mathbf{V}_h$ such that

$$\mathcal{N}'[\mathbf{u}_h](\mathbf{w}, \mathbf{z}_h) = J'[\mathbf{u}_h](\mathbf{w}) \quad \forall \mathbf{w} \in \mathbf{V}_h, \tag{10}$$

in adjoint residual form: Find $\mathbf{z}_h \in \mathbf{V}_h$ such that

$$\sum_{\kappa \in \mathcal{T}_h} \int_\kappa \mathbf{w} \cdot \mathbf{R}^*(\mathbf{z}_h) \, \mathrm{d}\mathbf{x} + \sum_{\kappa \in \mathcal{T}_h} \int_{\partial\kappa \setminus \Gamma} \mathbf{w} \cdot \mathbf{r}^*(\mathbf{z}_h) \, \mathrm{d}s + \int_\Gamma \mathbf{w} \cdot \mathbf{r}^*_\Gamma(\mathbf{z}_h) \, \mathrm{d}s \quad \forall \mathbf{w} \in V, \tag{11}$$

where $\mathbf{R}^*(\mathbf{z}_h)$, $\mathbf{r}^*(\mathbf{z}_h)$ and $\mathbf{r}^*_\Gamma(\mathbf{z}_h)$ denote the element, interior face and boundary adjoint residuals, respectively. According to (6), the discretization (4) is adjoint consistent if the exact solution $\mathbf{z}$ to (3) satisfies

$$\sum_{\kappa \in \mathcal{T}_h} \int_\kappa \mathbf{w} \cdot \mathbf{R}^*(\mathbf{z}) \, \mathrm{d}\mathbf{x} + \sum_{\kappa \in \mathcal{T}_h} \int_{\partial\kappa \setminus \Gamma} \mathbf{w} \cdot \mathbf{r}^*(\mathbf{z}) \, \mathrm{d}s + \int_\Gamma \mathbf{w} \cdot \mathbf{r}^*_\Gamma(\mathbf{z}) \, \mathrm{d}s \quad \forall \mathbf{w} \in V, \tag{12}$$

which holds if $\mathbf{z}$ satisfies

$$\mathbf{R}^*(\mathbf{z}) = 0 \ \text{ in } \kappa, \kappa \in \mathcal{T}_h, \qquad \mathbf{r}^*(\mathbf{z}) = 0 \ \text{ on } \partial\kappa \setminus \Gamma, \kappa \in \mathcal{T}_h, \qquad \mathbf{r}^*_\Gamma(\mathbf{z}) = 0 \ \text{ on } \Gamma.$$

Given a target functional of the form (2), we see that $\mathbf{R}^*(\mathbf{z}_h)$ depends on $j_\Omega(\cdot)$, and $\mathbf{r}^*_\Gamma(\mathbf{z}_h)$ depends on $j_\Gamma(\cdot)$. For obtaining adjoint consistent discretizations, it is, in some cases, see e.g. the following section, necessary to modify the target functional as follows

$$\tilde{J}(\mathbf{u}_h) = J(\mathbf{i}(\mathbf{u}_h)), \tag{13}$$

where $\mathbf{i}(\cdot)$ is a vector-valued function and will be specified in Section 3. A modification of a target functional is called *consistent* if $\tilde{J}(\mathbf{u}) = J(\mathbf{u})$ holds for the exact solution $\mathbf{u}$ to the primal problem (1). Thereby, the modification in (13) is consistent if the exact solution $\mathbf{u}$ satifies $\mathbf{i}(\mathbf{u}) = \mathbf{u}$. Although the true value of the target functional is unchanged, the computed value $J(\mathbf{u}_h)$ of the target functional is modified, and more importantly, $\tilde{J}'[\mathbf{u}_h]$ differs from $J'[\mathbf{u}_h]$. This modification can be used to recover an adjoint consistent discretization.

3. Adjoint consistency analysis for the discontinuous Galerkin discretization of the compressible Euler equations

In this section we consider the two-dimensional stationary compressible Euler equations

$$\nabla \cdot \mathcal{F}(\mathbf{u}) = 0 \quad \text{in } \Omega \subset \mathbb{R}^2, \tag{14}$$

subject to various boundary conditions, e.g. slip-wall boundary conditions at solid wall boundaries $\Gamma_W \subset \Gamma = \partial\Omega$, where a vanishing normal velocity

$$B\mathbf{u} = \mathbf{v} \cdot \mathbf{n} = v_1 n_1 + v_2 n_2 = 0 \quad \text{on } \Gamma_W \tag{15}$$

is imposed. In two space–dimensions, the vector of conservative variables $\mathbf{u}$ and the convective fluxes $\mathcal{F}(\mathbf{u}) = (\mathbf{f}_1(\mathbf{u}), \mathbf{f}_2(\mathbf{u}))$ are defined by

$$\mathbf{u} = \begin{bmatrix} \rho \\ \rho v_1 \\ \rho v_2 \\ \rho E \end{bmatrix}, \quad \mathbf{f}_1(\mathbf{u}) = \begin{bmatrix} \rho v_1 \\ \rho v_1^2 + p \\ \rho v_1 v_2 \\ \rho H v_1 \end{bmatrix} \text{ and } \mathbf{f}_2(\mathbf{u}) = \begin{bmatrix} \rho v_2 \\ \rho v_1 v_2 \\ \rho v_2^2 + p \\ \rho H v_2 \end{bmatrix},$$

where ρ, $\mathbf{v} = (v_1, v_2)^\top$, p and E denote the density, velocity vector, pressure and specific total energy, respectively. Additionally, H is the total enthalpy given by $H = E + \frac{p}{\rho} = e + \frac{1}{2}\mathbf{v}^2 + \frac{p}{\rho}$, where e is the specific static internal energy, and the pressure is determined by the equation of state of an ideal gas $p = (\gamma - 1)\rho e$, where $\gamma = c_p/c_v$ is the ratio of specific heat capacities at constant pressure, c_p, and constant volume, c_v; for dry air, $\gamma = 1.4$.

The most important target quantities in inviscid compressible flows are the pressure induced drag and lift coefficients, c_{dp} and c_{lp}, defined by

$$J(\mathbf{u}) = \int_\Gamma j(\mathbf{u})\,\mathrm{d}s = \frac{1}{C_\infty}\int_{\Gamma_W} p\,\mathbf{n}\cdot\psi\,\mathrm{d}s, \tag{16}$$

where $j(\mathbf{u}) = \frac{1}{C_\infty} p\,\mathbf{n}\cdot\psi$ on Γ_W and $j(\mathbf{u}) \equiv 0$ elsewhere. Here, $C_\infty = \frac{1}{2}\gamma p_\infty M_\infty^2 \bar{l} = \frac{1}{2}\gamma \frac{|\mathbf{v}_\infty|^2}{c_\infty^2} p_\infty \bar{l} = \frac{1}{2}\rho_\infty |\mathbf{v}_\infty|^2 \bar{l}$, where M denotes the Mach number, c the sound speed defined by $c^2 = \gamma p/\rho$, $\bar{l}$ denotes a reference length, and ψ is given by $\psi_d = (\cos(\alpha), \sin(\alpha))^\top$ or $\psi_l = (-\sin(\alpha), \cos(\alpha))^\top$ for the drag and lift coefficient, respectively. The subscripts $_\infty$ indicate free-stream quantities.

In order to derive the continuous adjoint problem, we multiply the left hand side of (14) by $\mathbf{z}$, integrate by parts and linearize about $\mathbf{u}$ to obtain

$$\left(\nabla \cdot \left(\mathcal{F}'[\mathbf{u}](\mathbf{w})\right), \mathbf{z}\right)_\Omega = -\left(\mathcal{F}'[\mathbf{u}](\mathbf{w}), \nabla\mathbf{z}\right)_\Omega + \left(\mathbf{n}\cdot\mathcal{F}'[\mathbf{u}](\mathbf{w}), \mathbf{z}\right)_\Gamma,$$

where $\mathcal{F}'[\mathbf{u}]$ denotes the Fréchet derivative of $\mathcal{F}$ with respect to $\mathbf{u}$. Thereby, the variational formulation of the continuous adjoint problem is given by: Find $\mathbf{z}$ such that

$$-\left(\mathbf{w}, \left(\mathcal{F}'[\mathbf{u}]\right)^\top \nabla\mathbf{z}\right)_\Omega + \left(\mathbf{w}, \left(\mathbf{n}\cdot\mathcal{F}'[\mathbf{u}]\right)^\top \mathbf{z}\right)_\Gamma = J'[\mathbf{u}](\mathbf{w}) \quad \forall \mathbf{w},$$

and the (continuous) adjoint solution $\mathbf{z}$ satisfies following problem in strong form

$$-\left(\mathcal{F}'[\mathbf{u}]\right)^\top \nabla \mathbf{z} = 0, \qquad \left(\mathbf{n}\cdot\mathcal{F}'[\mathbf{u}]\right)^\top \mathbf{z} = j'[\mathbf{u}] \quad \text{on } \Gamma. \tag{17}$$

Using $\mathcal{F}(\mathbf{u})\cdot\mathbf{n} = p(0,n_1,n_2,0)^\top$ on Γ_W, and the definition of $j(\cdot)$ in (16) we obtain

$$p'[\mathbf{u}](0,n_1,n_2,0)\cdot\mathbf{z} = \frac{1}{C_\infty} p'[\mathbf{u}]\mathbf{n}\cdot\psi \quad \text{on } \Gamma_W,$$

which reduces to the boundary conditions of the adjoint compressible Euler equations,

$$(B'[\mathbf{u}])^*\mathbf{z} = n_1 z_2 + n_2 z_3 = \frac{1}{C_\infty}\mathbf{n}\cdot\psi \quad \text{on } \Gamma_W. \tag{18}$$

Before introducing the DG discretization of (14) we define the finite element space $\mathbf{V}_h^p$ of discontinuous piecewise vector-valued polynomial functions of degree $p \geq 0$ by

$$\begin{aligned}\mathbf{V}_h^p = \{\mathbf{v}_h \in [L_2(\Omega)]^4 : \mathbf{v}_h|_\kappa \circ \sigma_\kappa \in [\mathcal{Q}_p(\hat\kappa)]^4 \text{ if } \hat\kappa \text{ is the unit hypercube, and} \\ \mathbf{v}_h|_\kappa \circ \sigma_\kappa \in [\mathcal{P}_p(\hat\kappa)]^4 \text{ if } \hat\kappa \text{ is the unit simplex}; \kappa \in \mathcal{T}_h\},\end{aligned}$$

where $\mathcal{Q}_p := \operatorname{span}\{\hat{\mathbf{x}}^\alpha : 0 \leq \alpha_i \leq p,\ 0 \leq i \leq d\}$ and $\mathcal{P}_p = \operatorname{span}\{\hat{\mathbf{x}}^\alpha : 0 \leq |\alpha| \leq p\}$. On interior edges $e = \partial\kappa \cap \partial\kappa'$ between two adjacent elements κ and κ', by $\mathbf{v}_\kappa^\pm$ ($\mathbf{v}^\pm$ for short) we denote the traces of $\mathbf{v}$ taken from within the interior of κ and κ', respectively. Furthermore, we define the jump of $\mathbf{u}$ by $\lfloor \mathbf{u} \rfloor = \mathbf{u}^+ - \mathbf{u}^-$.

Then, the discontinuous Galerkin discretization of (14) is given by: Find $\mathbf{u}_h \in \mathbf{V}_h^p$ such that

$$\begin{aligned}\mathcal{N}(\mathbf{u}_h,\mathbf{v}) \equiv -\int_\Omega \mathcal{F}(\mathbf{u}_h) : \nabla_h \mathbf{v}\,\mathrm{d}\mathbf{x} + \sum_{\kappa\in\mathcal{T}_h}\int_{\partial\kappa\setminus\Gamma} \mathcal{H}(\mathbf{u}_h^+,\mathbf{u}_h^-,\mathbf{n}^+)\,\mathbf{v}^+\,\mathrm{d}s \\ + \int_\Gamma \tilde{\mathcal{H}}(\mathbf{u}_h^+,\mathbf{u}_\Gamma(\mathbf{u}_h^+),\mathbf{n}^+)\,\mathbf{v}^+\,\mathrm{d}s = 0 \quad \forall \mathbf{v} \in \mathbf{V}_h^p,\end{aligned} \tag{19}$$

where $\mathcal{H}$ and $\tilde{\mathcal{H}}$ may be any Lipschitz continuous, consistent and conservative numerical flux functions, see e.g. [6], approximating the normal flux, $\mathbf{n}\cdot\mathcal{F}(\mathbf{u}_h)$. $\mathcal{H}$ takes into account the possible discontinuities of $\mathbf{u}_h$ at element interfaces. On the boundary Γ, $\tilde{\mathcal{H}}$ may depend on the interior trace $\mathbf{u}_h^+$ and a consistent boundary function $\mathbf{u}_\Gamma(\mathbf{u}_h^+)$. We note that $\tilde{\mathcal{H}}$ may be different from $\mathcal{H}$. In fact, we will see below, that depending on the specific choice of $\tilde{\mathcal{H}}$ the discontinuous Galerkin discretization (19) is adjoint consistent or not.

Using integration by parts we obtain equation (7) where the primal residuals are given by

$$\begin{aligned}\mathbf{R}(\mathbf{u}_h) &= -\nabla\cdot\mathcal{F}(\mathbf{u}_h) && \text{in } \kappa, \kappa\in\mathcal{T}_h, \\ \mathbf{r}(\mathbf{u}_h) &= \mathbf{n}\cdot\mathcal{F}(\mathbf{u}_h^+) - \mathcal{H}(\mathbf{u}_h^+,\mathbf{u}_h^-,\mathbf{n}^+) && \text{on } \partial\kappa\setminus\Gamma, \kappa\in\mathcal{T}_h, \\ \mathbf{r}_\Gamma(\mathbf{u}_h) &= \mathbf{n}\cdot\mathcal{F}(\mathbf{u}_h^+) - \tilde{\mathcal{H}}(\mathbf{u}_h^+,\mathbf{u}_\Gamma(\mathbf{u}_h^+),\mathbf{n}^+) && \text{on } \Gamma.\end{aligned} \tag{20}$$

Given the consistency of the numerical flux, $\mathcal{H}(\mathbf{w},\mathbf{w},\mathbf{n}) = \mathbf{n}\cdot\mathcal{F}(\mathbf{w})$, and the consistency of the boundary function, i.e. $\mathbf{u}_\Gamma(\mathbf{u}) = \mathbf{u}$ for the exact solution $\mathbf{u}$ to (14), we find that $\mathbf{u}$ satifies

$$\mathbf{R}(\mathbf{u}) = 0 \ \text{ in } \kappa,\kappa\in\mathcal{T}_h, \qquad \mathbf{r}(\mathbf{u}) = 0 \ \text{ on } \partial\kappa\setminus\Gamma, \kappa\in\mathcal{T}_h, \qquad \mathbf{r}_\Gamma(\mathbf{u}) = 0 \ \text{ on } \Gamma. \tag{21}$$

We conclude that (19) is a consistent discretization of (14).

Given the target functional $J(\cdot)$ defined in (16) with Fréchet derivative, $J'[\mathbf{u}](\cdot)$, the discrete adjoint problem is given by (10), where

$$\begin{aligned}\mathcal{N}'[\mathbf{u}_h](\mathbf{w},\mathbf{z}_h) \equiv -\int_\Omega \left(\mathcal{F}'[\mathbf{u}_h]\mathbf{w}\right) : \nabla_h \mathbf{z}_h\,\mathrm{d}\mathbf{x} \\ + \sum_{\kappa\in\mathcal{T}_h}\int_{\partial\kappa\setminus\Gamma} \left(\mathcal{H}'_{\mathbf{u}^+}(\mathbf{u}_h^+,\mathbf{u}_h^-,\mathbf{n}^+)\mathbf{w}^+ + \mathcal{H}'_{\mathbf{u}^-}(\mathbf{u}_h^+,\mathbf{u}_h^-,\mathbf{n}^+)\mathbf{w}^-\right)\mathbf{z}_h^+\,\mathrm{d}s \\ + \int_\Gamma \left(\tilde{\mathcal{H}}'_{\mathbf{u}^+}\left(\mathbf{u}_h^+,\mathbf{u}_\Gamma(\mathbf{u}_h^+),\mathbf{n}^+\right) + \tilde{\mathcal{H}}'_{\mathbf{u}^-}\left(\mathbf{u}_h^+,\mathbf{u}_\Gamma(\mathbf{u}_h^+),\mathbf{n}^+\right)\mathbf{u}'_\Gamma(\mathbf{u}_h^+)\right)\mathbf{w}^+\mathbf{z}_h^+\,\mathrm{d}s.\end{aligned} \tag{22}$$

Here $\mathbf{v} \to \mathcal{H}'_{\mathbf{u}^+}(\mathbf{v}^+, \mathbf{v}^-, \mathbf{n})$ and $\mathbf{v} \to \mathcal{H}'_{\mathbf{u}^-}(\mathbf{v}^+, \mathbf{v}^-, \mathbf{n})$ denote the derivatives of the flux function $\mathcal{H}(\cdot,\cdot,\cdot)$ with respect to its first and second arguments, respectively. From the conservativity of the numerical flux, $\mathcal{H}(\mathbf{v},\mathbf{w},\mathbf{n}) = -\mathcal{H}(\mathbf{w},\mathbf{v},-\mathbf{n})$, we conclude

$$\mathcal{H}'_{\mathbf{u}^-}(\mathbf{v},\mathbf{w},\mathbf{n}) = \frac{\partial}{\partial \mathbf{w}}\mathcal{H}(\mathbf{v},\mathbf{w},\mathbf{n}) = -\frac{\partial}{\partial \mathbf{w}}\mathcal{H}(\mathbf{w},\mathbf{v},-\mathbf{n}) = -\mathcal{H}'_{\mathbf{u}^+}(\mathbf{w},\mathbf{v},-\mathbf{n}).$$

Using this, the discrete adjoint problem (10) is rewritten as follows: Find $\mathbf{z}_h \in \mathbf{V}_h^p$ such that

$$\begin{aligned} -\int_\Omega \left(\mathcal{F}'[\mathbf{u}_h]\mathbf{w}\right) : \nabla_h \mathbf{z}_h \,\mathrm{d}\mathbf{x} + \sum_{\kappa\in\mathcal{T}_h} \int_{\partial\kappa\setminus\Gamma} \mathcal{H}'_{\mathbf{u}^+}(\mathbf{u}_h^+, \mathbf{u}_h^-, \mathbf{n}^+)\mathbf{w}^+ \lfloor \mathbf{z}_h \rfloor \,\mathrm{d}s \\ + \int_\Gamma \left(\tilde{\mathcal{H}}'_{\mathbf{u}^+}\left(\mathbf{u}_h^+, \mathbf{u}_\Gamma(\mathbf{u}_h^+), \mathbf{n}^+\right) + \tilde{\mathcal{H}}'_{\mathbf{u}^-}\left(\mathbf{u}_h^+, \mathbf{u}_\Gamma(\mathbf{u}_h^+), \mathbf{n}^+\right) \mathbf{u}'_\Gamma(\mathbf{u}_h^+) \right) \mathbf{w}^+ \mathbf{z}_h^+ \,\mathrm{d}s = J'[\mathbf{u}_h](\mathbf{w}), \end{aligned}$$

for all $\mathbf{w} \in \mathbf{V}_h^p$. We see that the discrete adjoint solution $\mathbf{z}_h$ must satisfy following problem

$$-(\mathcal{F}'[\mathbf{u}])^\top \nabla \mathbf{z} = 0 \quad \text{in } \kappa, \kappa \in \mathcal{T}_h, \tag{23}$$

subject to inter-element conditions

$$\left(\mathcal{H}'_{\mathbf{u}^+}(\mathbf{u}^+, \mathbf{u}^-, \mathbf{n}^+)\right)^\top \lfloor \mathbf{z} \rfloor = 0 \quad \text{on } \partial\kappa \setminus \Gamma, \kappa \in \mathcal{T}_h, \tag{24}$$

and boundary conditions

$$\left(\tilde{\mathcal{H}}'_{\mathbf{u}^+} + \tilde{\mathcal{H}}'_{\mathbf{u}^-}\mathbf{u}'_\Gamma(\mathbf{u})\right)^\top \mathbf{z} = j'[\mathbf{u}] \quad \text{on } \Gamma, \tag{25}$$

where $\tilde{\mathcal{H}}'_{\mathbf{u}^+} := \tilde{\mathcal{H}}'_{\mathbf{u}^+}(\mathbf{u}^+, \mathbf{u}_\Gamma(\mathbf{u}^+), \mathbf{n}^+)$ and $\tilde{\mathcal{H}}'_{\mathbf{u}^-} := \tilde{\mathcal{H}}'_{\mathbf{u}^-}(\mathbf{u}^+, \mathbf{u}_\Gamma(\mathbf{u}^+), \mathbf{n}^+)$.

Comparing the discrete adjoint boundary condition (25) and the continuous adjoint boundary condition in (17), we see, that not all choices for $\tilde{\mathcal{H}}$ give rise to an adjoint consistent discretization. In fact, we require $\tilde{\mathcal{H}}$ to have following properties: In order to incorporate boundary conditions in the primal discretization (19), $\tilde{\mathcal{H}}$ must depend on $\mathbf{u}_\Gamma(\mathbf{u}^+)$, hence $\tilde{\mathcal{H}}'_{\mathbf{u}^-} \neq 0$. Furthermore, we require $\tilde{\mathcal{H}}'_{\mathbf{u}^+} = 0$, as otherwise the left hand side of (25) involves two summands which is in contrast to (17). Finally, we recall that $\tilde{\mathcal{H}}$ is consistent, $\tilde{\mathcal{H}}(\mathbf{v},\mathbf{v},\mathbf{n}) = \mathbf{n}\cdot\mathcal{F}(\mathbf{v})$, and conclude that $\tilde{\mathcal{H}}$ is given by $\tilde{\mathcal{H}}(\mathbf{u}_h^+, \mathbf{u}_\Gamma(\mathbf{u}_h^+), \mathbf{n}) = \mathbf{n}\cdot\mathcal{F}(\mathbf{u}_\Gamma(\mathbf{u}_h^+))$. Employing a modified target functional $\tilde{J}(\mathbf{u}_h) = J(\mathbf{i}(\mathbf{u}_h))$, (25) yields

$$\left(\mathbf{n}\cdot\left(\mathcal{F}'[\mathbf{u}_\Gamma(\mathbf{u}_h^+)]\right)\mathbf{u}'_\Gamma(\mathbf{u}_h^+)\right)^\top \mathbf{z} = j'[\mathbf{i}(\mathbf{u}_h^+)]\mathbf{i}'(\mathbf{u}_h^+). \tag{26}$$

We find the modification $i(\mathbf{u}_h) = \mathbf{u}_\Gamma(\mathbf{u}_h)$ which is consistent as $i(\mathbf{u}) = \mathbf{u}_\Gamma(\mathbf{u}) = \mathbf{u}$ holds for the exact solution $\mathbf{u}$. Thereby (26) reduces to

$$\left(\mathbf{n}\cdot\mathcal{F}'[\mathbf{u}_\Gamma(\mathbf{u}_h^+)]\right)^\top \mathbf{z} = j'[\mathbf{u}_\Gamma(\mathbf{u}_h^+)], \tag{27}$$

which represents a discretization of the continuous adjoint boundary condition in (17). In order to obtain a discretization of the adjoint boundary condition at solid wall boundaries (18), we require $B\mathbf{u}_\Gamma(\mathbf{u}_h^+) = 0$ on Γ_W. This condition is satisfied by

$$\mathbf{u}_\Gamma(\mathbf{u}) = \begin{pmatrix} 1 & 0 & 0 & 0 \\ 0 & 1-n_1^2 & -n_1n_2 & 0 \\ 0 & -n_1n_2 & 1-n_2^2 & 0 \\ 0 & 0 & 0 & 1 \end{pmatrix} \mathbf{u} \quad \text{on} \quad \Gamma_W, \tag{28}$$

which originates from $\mathbf{u}$ by subtracting the normal velocity component of $\mathbf{u}$, i.e. $\mathbf{v} = (v_1, v_2)$ is replaced by $\mathbf{v}_\Gamma = \mathbf{v} - (\mathbf{v}\cdot\mathbf{n})\mathbf{n}$ which ensures that the normal velocity component vanishes, $\mathbf{v}_\Gamma \cdot \mathbf{n} = 0$. In summary, let $\mathbf{u}_\Gamma$ be given by (28) and $\tilde{\mathcal{H}}$ and $\tilde{J}$ be defined by

$$\tilde{\mathcal{H}}(\mathbf{u}_h^+, \mathbf{u}_\Gamma(\mathbf{u}_h^+), \mathbf{n}) = \mathbf{n}\cdot\mathcal{F}_\Gamma(\mathbf{u}_h^+), \qquad \tilde{J}(\mathbf{u}_h) = J_\Gamma(\mathbf{u}_h), \tag{29}$$

where $\mathcal{F}_\Gamma(\mathbf{u}_h^+) := \mathcal{F}(\mathbf{u}_\Gamma(\mathbf{u}_h^+))$, $J_\Gamma(\mathbf{u}_h) := J(\mathbf{u}_\Gamma(\mathbf{u}_h))$ and $j_\Gamma(\mathbf{u}_h) := j(\mathbf{u}_\Gamma(\mathbf{u}_h))$, then the discrete adjoint problem (30) is given by: Find $\mathbf{z}_h \in \mathbf{V}_h^p$ such that

$$\begin{aligned} -\int_\Omega \big(\mathcal{F}'[\mathbf{u}_h](\mathbf{w})\big) : \nabla_h \mathbf{z}_h \,\mathrm{d}\mathbf{x} + \sum_{\kappa\in\mathcal{T}_h} \int_{\partial\kappa\setminus\Gamma} \mathcal{H}'_{\mathbf{u}^+}(\mathbf{u}_h^+, \mathbf{u}_h^-, \mathbf{n}^+)\mathbf{w}^+[\mathbf{z}_h]\,\mathrm{d}s \\ + \int_\Gamma \left(\mathbf{n}\cdot\mathcal{F}'_\Gamma[\mathbf{u}_h^+]\right)\mathbf{w}^+\mathbf{z}_h^+ \,\mathrm{d}s = J'_\Gamma[\mathbf{u}_h](\mathbf{w}), \end{aligned} \tag{30}$$

for all $\mathbf{w} \in \mathbf{V}_h^p$. Hence, we have (11) where the adjoint residuals are given by

$$\begin{aligned} \mathbf{R}^*(\mathbf{z}_h) &= (\mathcal{F}'[\mathbf{u}])^\top \nabla \mathbf{z}_h && \text{in } \kappa, \kappa\in\mathcal{T}_h, \\ \mathbf{r}^*(\mathbf{z}_h) &= -\left(\mathcal{H}'_{\mathbf{u}^+}(\mathbf{u}^+, \mathbf{u}^-, \mathbf{n}^+)\right)^\top \lfloor \mathbf{z}_h \rfloor && \text{on } \partial\kappa\setminus\Gamma, \kappa\in\mathcal{T}_h, \\ \mathbf{r}^*_\Gamma(\mathbf{z}_h) &= \left(j'_\Gamma[\mathbf{u}_h^+] - \mathbf{n}\cdot\mathcal{F}'_\Gamma[\mathbf{u}_h^+]\right)^\top \mathbf{z}_h^+ && \text{on } \Gamma. \end{aligned} \tag{31}$$

In particular, the discretization (19) together with (29) is adjoint consistent as the exact solution $\mathbf{z}$ to the continuous adjoint problem (17) satifies

$$\mathbf{R}^*(\mathbf{z}) = 0 \ \text{ in } \kappa, \kappa\in\mathcal{T}_h, \qquad \mathbf{r}^*(\mathbf{z}) = 0 \ \text{ on } \partial\kappa\setminus\Gamma, \kappa\in\mathcal{T}_h, \qquad \mathbf{r}^*_\Gamma(\mathbf{z}) = 0 \ \text{ on } \Gamma. \tag{32}$$

We note, that the standard discontinuous Galerkin discretizations of the compressible Euler equations, see e.g. [2, 6, 7] among several others, take the same numerical flux function on the boundary Γ as in the interior of the domain, and simply replace $\mathbf{u}_h^-$ in $\mathcal{H}(\mathbf{u}_h^+, \mathbf{u}_h^-, \mathbf{n})$ by the boundary function $\mathbf{u}_\Gamma(\mathbf{u}_h^+)$ resulting in $\tilde{\mathcal{H}}(\mathbf{u}_h^+, \mathbf{u}_\Gamma(\mathbf{u}_h^+), \mathbf{n})$. Furthermore, the definition of $\mathbf{u}_\Gamma$ in e.g. [2, 6] based on $\mathbf{v}_\Gamma = \mathbf{v} - 2(\mathbf{v}\cdot\mathbf{n})\mathbf{n}$ ensures a vanishing average normal velocity, $\bar{\mathbf{v}}\cdot\mathbf{n} = \frac{1}{2}(\mathbf{v}+\mathbf{v}_\Gamma)\cdot\mathbf{n} = 0$. However, $\mathbf{v}_\Gamma\cdot\mathbf{n} = 0$ and $B\mathbf{u}_\Gamma(\mathbf{u}_h^+) = 0$, as required in (27), is not satisfied. Thereby, the discontinuous Galerkin discretization based on the standard choice of $\tilde{\mathcal{H}}$ and $\mathbf{u}_\Gamma$ is not adjoint consistent. In fact, already [6] noticed large gradients, i.e. an irregular adjoint solution, near solid wall boundaries. Recently, in [9], it has been demonstrated for an inviscid compressible flow over a bump, that a discretization based on (29) is adjoint consistent and gives rise to a smooth adjoint solution.

4. Numerical experiments

In this section, we will demonstrate the effect on the smoothness of the discrete adjoint solution when employing the adjoint consistent discretization based on (29) in comparison to the standard (classical) approach of choosing $\tilde{\mathcal{H}}(\mathbf{u}_h^+, \mathbf{u}_\Gamma(\mathbf{u}_h^+), \mathbf{n})$ and an unmodified target functional $J(\mathbf{u}_h)$. Furthermore, we show the effect of the smoothness of the adjoint solution on the a posteriori error estimation, see [6]. To this end, we revisit the $M = 0.5$, $\alpha = 0^\circ$ inviscid flow around the NACA0012 airfoil test case considered in [6]. In Figure 1 we compare the (primal) flow solutions $\mathbf{u}_h \in \mathbf{V}_h^1$ for the standard and the adjoint consistent DG discretizations and find no visible difference. However, when comparing the adjoint solutions, see Figure 2, we notice that the discrete adjoint solution to the standard DG discretization is irregular near and upstream the airfoil. In contrast to that, the adjoint solution to the adjoint consistent discretization is entirely smooth.

In Tables 1 and 2 we collect the data of a goal-oriented (adjoint-based) adaptive refinement algorithm, [6], tailored to the accurate computation of the drag coefficient, c_{dp}, for the standard

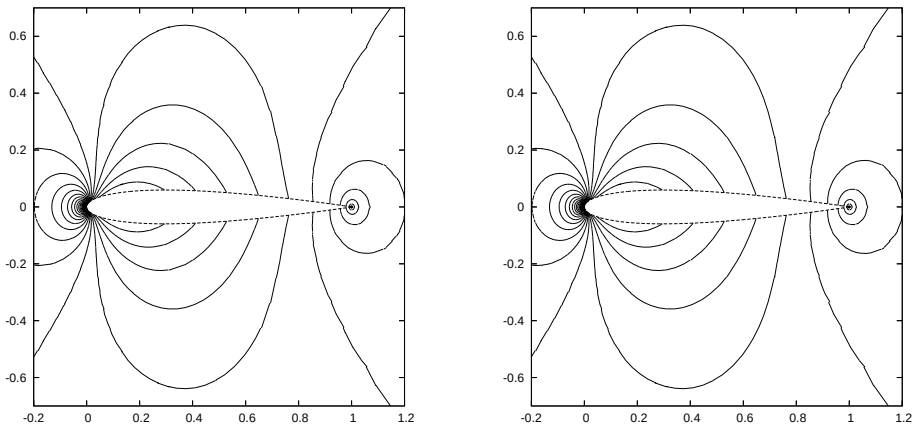

Figure 1: $M = 0.5, \alpha = 0^\circ$ inviscid flow around the NACA0012 airfoil: Mach isolines of the (primal) flow solution $\mathbf{u}_h$ to (left) the standard and (right) the adjoint-consistent DG discretization.

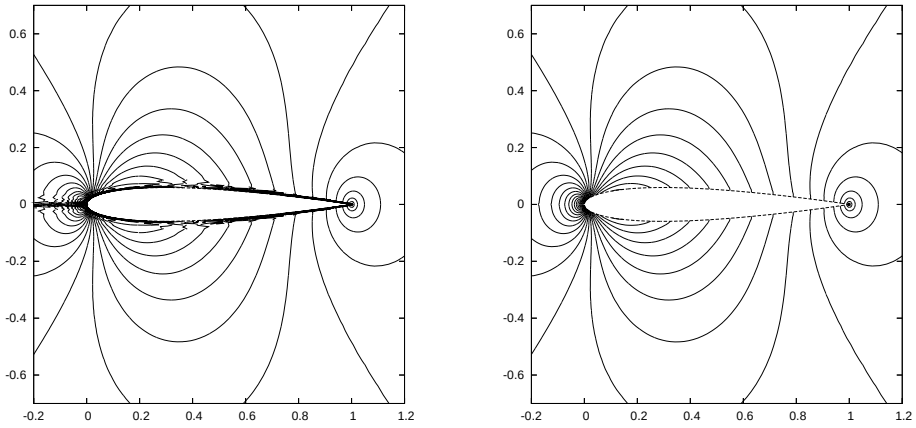

Figure 2: $M = 0.5, \alpha = 0^\circ$ inviscid flow around the NACA0012 airfoil: z_1 isolines of the discrete adjoint solution $\mathbf{z}_h$ to (left) the standard and (right) the adjoint-consistent DG discretization.

and the adjoint-consistent DG discretization, respectively. Here, we show the number of elements and degrees of freedom, the true error $J(\mathbf{u}) - J(\mathbf{u}_h)$ based on the true value $J(\mathbf{u}) = 0$, the estimated error based on the approximate error representation $\eta = -\mathcal{N}(\mathbf{u}_h, \mathbf{z}_h) = \sum_\kappa \eta_\kappa$ with $\mathbf{z}_h \in \mathbf{V}_h^2$, and the value $\tilde{\eta} = \sum_\kappa |\eta_\kappa|$ after applying the triangular inequality, together with the corresponding effectivity indices $\theta_1 = \eta / |J(\mathbf{u}) - J(\mathbf{u}_h)|$ and $\theta_2 = \tilde{\eta} / |J(\mathbf{u}) - J(\mathbf{u}_h)|$. Whereas both histories of adaptively refined meshes are almost identical, we see that on all corresponding meshes the adjoint-consistent discretization is by a factor of about 1.3-2.4 more accurate than the standard DG discretization. Furthermore, we see that in both cases the error estimation is quite accurate represented by the fact that θ_1 is close to one. The error estimation for the adjoint-consistent discretization is improved on coarser grid but slightly degraded on finer meshes in comparison to the standard DG discretization. Finally, θ_1 and θ_2 in Table 1 differ, indicating that the standard DG discretization causes an extensive error cancellation, which is also seen in the irregular adjoint solution. In contrast to that the adjoint solution to the adjoint consistent DG discretization is smooth, no cancellation effects occur and θ_1 and θ_2 in Table 2 coincide.

5. Concluding remarks

In this article, we have provided a general framework for analyzing adjoint consistency for DG discretizations, introduced consistent modifications of target functionals, and derived an adjoint

# cells	# dofs	$J(\mathbf{u}) - J(\mathbf{u}_h)$	$\eta = \sum_\kappa \eta_\kappa$	θ_1	$\tilde{\eta} = \sum_\kappa \lvert\eta_\kappa\rvert$	θ_2
768	12288	-5.008e-03	-3.279e-03	0.65	7.290e-03	-1.46
1242	19872	-1.783e-03	-1.531e-03	0.86	3.875e-03	-2.17
2061	32976	-5.422e-04	-5.206e-04	0.96	1.382e-03	-2.5
3339	53424	-1.617e-04	-1.632e-04	1.01	4.792e-04	-2.96
5535	88560	-5.060e-05	-5.270e-05	1.04	1.639e-04	-3.24

Table 1: *A posteriori* error estimation for the standard DG discretization.

# cells	# dofs	$J(\mathbf{u}) - J(\mathbf{u}_h)$	$\eta = \sum_\kappa \eta_\kappa$	θ_1	$\tilde{\eta} = \sum_\kappa \lvert\eta_\kappa\rvert$	θ_2
768	12288	-3.800e-03	-3.267e-03	0.86	3.270e-03	0.86
1242	19872	-8.833e-04	-8.352e-04	0.95	8.376e-04	0.95
2022	32352	-2.302e-04	-2.139e-04	0.93	2.150e-04	0.93
3327	53232	-8.405e-05	-7.607e-05	0.91	7.658e-05	0.91
5577	89232	-3.754e-05	-3.369e-05	0.90	3.392e-05	0.90

Table 2: *A posteriori* error estimation for the adjoint-consistent DG discretization.

consistent discontinuous Galerkin discretization for the compressible Euler equations originally proposed in [9]. Numerical experiments have demonstrated the effect of adjoint consistency on the smoothness of discrete adjoint solutions and on the *a posteriori* error estimation on locally refined meshes. Future research [5] will be dedicated to the adjoint consistency analysis of the interior penalty DG discretization of the compressible Navier-Stokes equations [7].

References

[1] D. Arnold, F. Brezzi, B. Cockburn, and D. Marini. Unified analysis of discontinuous Galerkin methods for elliptic problems. *SIAM J. Numer. Anal.*, 39(5):1749–1779, 2002.

[2] F. Bassi and S. Rebay. High-order accurate discontinuous finite element solution of the 2d Euler equations. *J. Comp. Phys.*, 138:251–285, 1997.

[3] K. Harriman, D. Gavaghan, and E. Süli. The importance of adjoint consistency in the approximation of linear functionals using the discontinuous Galerkin finite element method. Technical report, Oxford University Computing Laboratory, 2004.

[4] K. Harriman, P. Houston, B. Senior, and E. Süli. *hp*–Version discontinuous Galerkin methods with interior penalty for partial differential equations with nonnegative characteristic form. In *Recent Advances in Scientific Computing and Partial Differential Equations*, volume 330 of *Contemporary Mathematics*, pages 89–119. AMS, 2003.

[5] R. Hartmann. Adjoint consistency analysis of discontinuous Galerkin discretizations. *SIAM J. Numer. Anal.*, 2006. in preparation.

[6] R. Hartmann and P. Houston. Adaptive discontinuous Galerkin finite element methods for the compressible Euler equations. *J. Comp. Phys.*, 183:508–532, 2002.

[7] R. Hartmann and P. Houston. Symmetric interior penalty DG methods for the compressible Navier–Stokes equations I: Method formulation. *Int. J. Num. Anal. Model.*, 3(1):1–20, 2006.

[8] P. Houston, R. Rannacher, and E. Süli. A posteriori error analysis for stabilised finite element approximations of transport problems. *Comput. Meth. Appl. Mech. Engrg.*, 190(11-12):1483–1508, 2000.

[9] J. Lu and D. L. Darmofal. Dual-consistency analysis and error estimation for discontinuous Galerkin discretization: application to first-order conservation laws. *IMA Journal of Numerical Analysis*, 2006. submitted.